Science Robotics
AAAS

robotics.sciencemag.org/cgi/content/full/5/46/eabb0467/DC1

Supplementary Materials for

The Hannes hand prosthesis replicates the key biological properties of the human hand

M. Laffranchi*, N. Boccardo, S. Traverso, L. Lombardi, M. Canepa, A. Lince, M. Semprini, J. A. Saglia, A. Naceri, R. Sacchetti, E. Gruppioni, L. De Michieli

*Corresponding author. Email: matteo.laffranchi@iit.it

Published 23 September 2020, *Sci. Robot.* **5**, eabb0467 (2020)
DOI: 10.1126/scirobotics.abb0467

The PDF file includes:

Text S1. Mechanical model
Text S2. Angle extraction
Fig. S1. First three synergies.
Fig. S2. The three stable rotation positions of the thumb.
Fig. S3. Outline of the experimental protocol.
Fig. S4. Forces acting in the palm mechanism.
Fig. S5. Mechanics of the digits.
Table S1. The main dimensions of the digits of the human hand and Hannes.
Table S2. Scores of the tests and questionnaires.
Table S3. Final evaluation questionnaire.
Table S4. Comparison table of commercial and research prosthetic hands.
Table S5. Participants' information.
Table S6. ADL tasks executed during the rehabilitative training with Hannes.
Legends for movies S1 and S2
References (*74–76*)

Other Supplementary Material for this manuscript includes the following:

(available at robotics.sciencemag.org/cgi/content/full/5/46/eabb0467/DC1)

Movie S1 (.mp4 format). Amputees performing clinical tests with Hannes.
Movie S2 (.mp4 format). Healthy participants performing precision and lateral grasps with Hannes.

Supplementary Text

Text S1. Mechanical model

Poly-articulated hand

Consider the pulling force F_A acting on the idle pulley located on the leader wire side of one of the custom-made bush bearings, Fig. S4A. This force generates two reaction forces on the other idle pulley F_A^{2k-1} and F_A^{2k}, where $k = \{1, 2\}$ identifies the follower wire: *k=1* represents follower 1, whereas *k=2* identifies the second follower wire, as shown in Fig. S4B. Considering this differential mechanism, it is possible to define the force transmission matrix $\boldsymbol{T}_k$ that relates the actuation force to the force generated by the wires routed into the two finger pairs, the index-middle and ring-little fingers:

$$\boldsymbol{F}_{A,k} = \begin{bmatrix} F_A^{2k-1} \\ F_A^{2k} \end{bmatrix} = \begin{bmatrix} \dfrac{r_b}{(r_a + r_b)} \\ \dfrac{r_a}{(r_a + r_b)} \end{bmatrix} 2\, F_A = \boldsymbol{T}_k\, F_A \tag{1}$$

$\boldsymbol{F}_{A,k}$ is an array containing the forces applied to each of the two finger pairs. In this array, forces are identified so that F_A^1 corresponds to the force applied to the index finger and F_A^4 that applied to the little, Fig. S4A. As r_a is equal to r_b, the following can be derived from equation (1):

$$\boldsymbol{T}_k = \begin{bmatrix} 1 \\ 1 \end{bmatrix} \tag{2}$$

As the force generated in the wire that actuates the thumb (i.e., the leader wire) is F_A, it follows that by applying equation (1) to all the digits, the full transmission matrix $[\boldsymbol{S}_{hand}]_{5x1}$ that relates the actuation force F_A to the vector of forces applied to all the actuating digits' wires, $\boldsymbol{F}_A$ is:

$$\boldsymbol{F}_A = \boldsymbol{S}_{hand}\, F_A = \begin{bmatrix} \boldsymbol{T}_1 \\ \boldsymbol{T}_2 \\ 1 \end{bmatrix} F_A \tag{3}$$

where the last element of $\boldsymbol{S}_{hand}$ equals one due to the considerations made for the thumb in the materials and methods section. Neglecting friction effects, equation (3) states that each of the elements in $\boldsymbol{F}_A$ equal the actuation force F_A. Thus, the force delivered to the digits is always uniformly distributed among them, regardless of the operating state of the device. It results that $\boldsymbol{S}_{hand}$ is an all-ones matrix:

$$\boldsymbol{S}_{hand} = [1]_{5x1} \tag{4}$$

Fingers

Considering the detailed mechanical scheme in Fig. S5A, the following equation describes the equilibrium of the torques around the MCP joint and relates the interaction forces R_i^j with the follower wire forces F_A^j and angles of the j-th digit:

$$\sum_{i=1}^{n} R_i^j b_i^j\left(\theta_{PIP}^j\right) = F_A^j h^j\left(\theta_{MCP}^j\right) + f^j n^j\left(\theta_{PIP}^j\right) + F_A^j a^j\left(\theta_{PIP}^j\right) - f^j y^j\left(\theta_{MCP}^j\right)$$

$$\sum_{i=1}^{n} R_i^j b_i^j\left(\theta_{PIP}^j\right) = F_A^j \left(h^j\left(\theta_{MCP}^j\right) + a^j\left(\theta_{PIP}^j\right)\right) + f^j \left(n^j\left(\theta_{PIP}^j\right) - y^j\left(\theta_{MCP}^j\right)\right) \quad (5)$$

$$\begin{Bmatrix} R_1^j & \cdots & R_n^j \end{Bmatrix} \begin{Bmatrix} b_1^j\left(\theta_{PIP}^j\right) \\ \cdots \\ b_n^j\left(\theta_{PIP}^j\right) \end{Bmatrix} = \begin{Bmatrix} F_A^j & f^j \end{Bmatrix} \begin{Bmatrix} h^j\left(\theta_{MCP}^j\right) + a^j\left(\theta_{PIP}^j\right) \\ n^j\left(\theta_{PIP}^j\right) - y^j\left(\theta_{MCP}^j\right) \end{Bmatrix}$$

where b_i^j represents the lever arm relative to the point of the application of the interaction forces R_i^j and the MCP joint and f^j is the force generated by the return wire. θ_{MCP}^j and θ_{PIP}^j are the MCP and PIP joint angles, respectively. The parameters $h^j\left(\theta_{MCP}^j\right)$, $a^j\left(\theta_{PIP}^j\right)$, $n^j\left(\theta_{PIP}^j\right)$ and $y^j\left(\theta_{MCP}^j\right)$ are the lever arms upon which the internal forces F_A^j and f^j act to generate torque on the MCP and PIP joints, respectively.

The mechanical interface between the fingers and palm allows passive abduction/adduction movement to accommodate the finger configurations during grasping. These mechanisms are made of custom hinges provided with rubber inserts, allowing an elastic range of motion of ±5°.

Thumb

Equation (5) is also valid for this digit; however, θ_{MCP}^j is replaced by θ_{ABD}, and θ_{PIP}^j disappears because it is constant and independent of the abduction and rotation positions. As θ_{PIP}^j is constant, the computation of the torque around the abduction joint does not involve the terms $a^j\left(\theta_{PIP}^j\right)$ and $n^j\left(\theta_{PIP}^j\right)$. This results in the following torque equilibrium for the thumb (Fig. S5B):

$$\begin{Bmatrix} R_1^5 & \cdots & R_n^5 \end{Bmatrix} \begin{Bmatrix} b_1^5 \\ \cdots \\ b_n^5 \end{Bmatrix} = \begin{Bmatrix} F_A^5 & f^5 \end{Bmatrix} \begin{Bmatrix} h^5(\theta_{ABD}) \\ -y^5(\theta_{ABD}) \end{Bmatrix} \quad (6)$$

Text S2. Angles extraction

The trajectories of each marker in the space were acquired and reconstructed using Vicon software (Nexus 2.8.1). Missing data or faulty reconstructions were interpolated using a suitable interpolation method: linear interpolation for gaps of < 50 ms; cubic spline interpolation with a continuous first derivative for gaps of < 100 ms; and an adaptive NLM filter native in the Nexus Environment trained for larger gaps, assuming sufficient trajectory was available to train the algorithm. The entire dataset was low-pass filtered (4^{th}-order Cauer filter with zero lag, -60 dB attenuation and a 10 Hz cut-off frequency) and fed into the MATLAB pipeline. The raw trajectory data were windowed as identified by the trial duration. The start of the trial was defined as the time frame in which any of the markers changed their position by more than three times the observed "static" noise level. Analogously, the end frame was defined as the last frame at which all markers were below the aforementioned threshold. The 20 joint angles were estimated from the spatial positions of the marker set through an established kinematic model of the human hand (Fig. 3B) to allow a direct comparison with previous studies (*48*). For each finger, the DIP

and PIP joint angles were calculated by reconstructing the axes of the phalanxes from the relative marker position. MCP flexion and abduction relied on regression based on closed-form inverse kinematics. The thumb angles were also calculated directly by reconstructing the axes of the phalanxes. This process was repeated for each time frame. The joint space trajectories were scanned for plateaus, and the values were collected into a posture vector belonging to $\mathbb{R}^{20}$ (according to the kinematic model in Fig. 3B). The process was repeated for each object and participant. All human posture vectors were collected into a single set.

Supplementary Figures

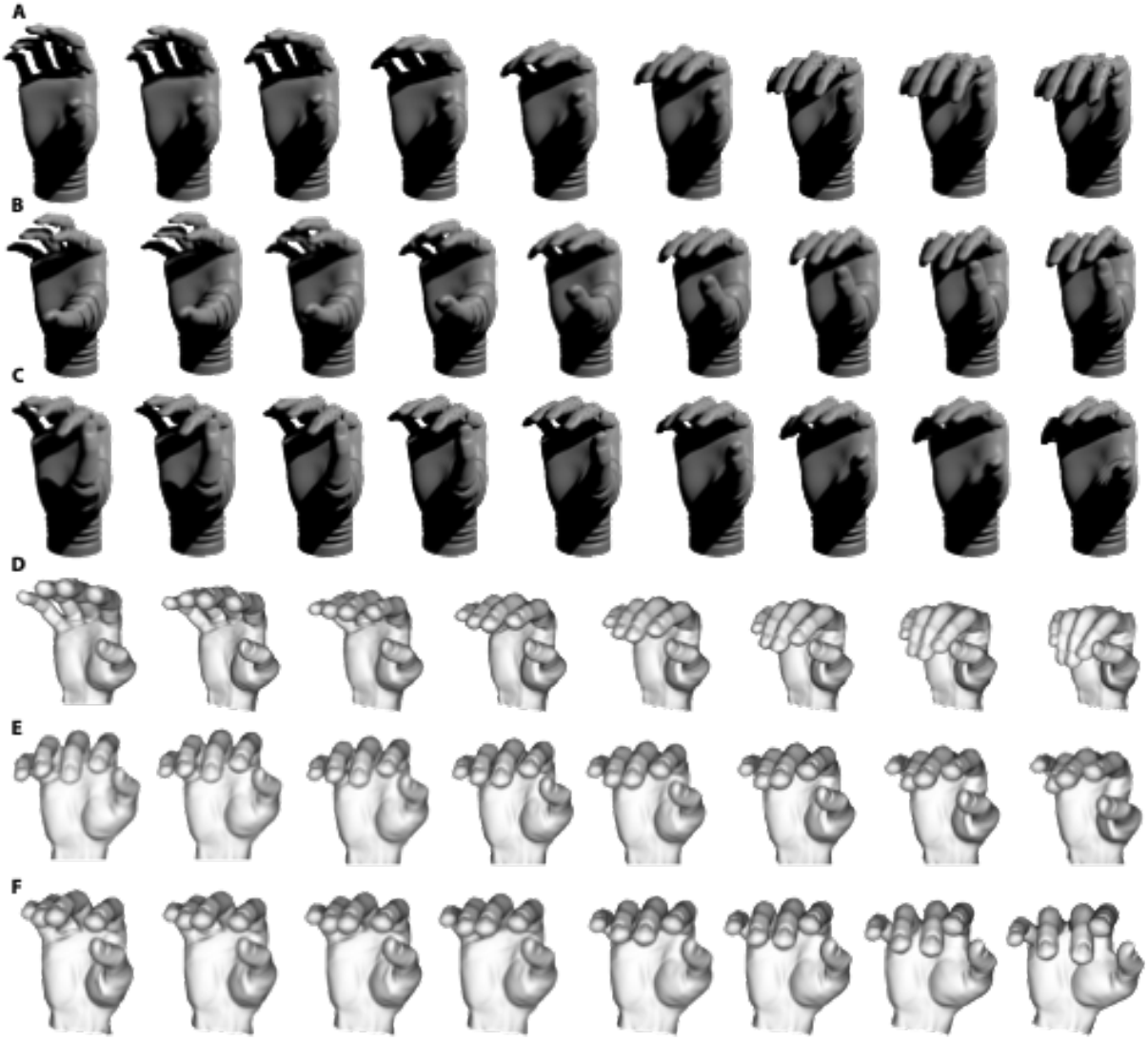

Fig. S1. First three synergies. From top to bottom: Hannes (**A**) PC1, (**B**) PC2 and (**C**) PC3 and the human hand (**D**) PC1, (**E**) PC2 and (**F**) PC3 over the range of the minimum and maximum observed scores ((*73*) credited for the mesh model of the human hand).

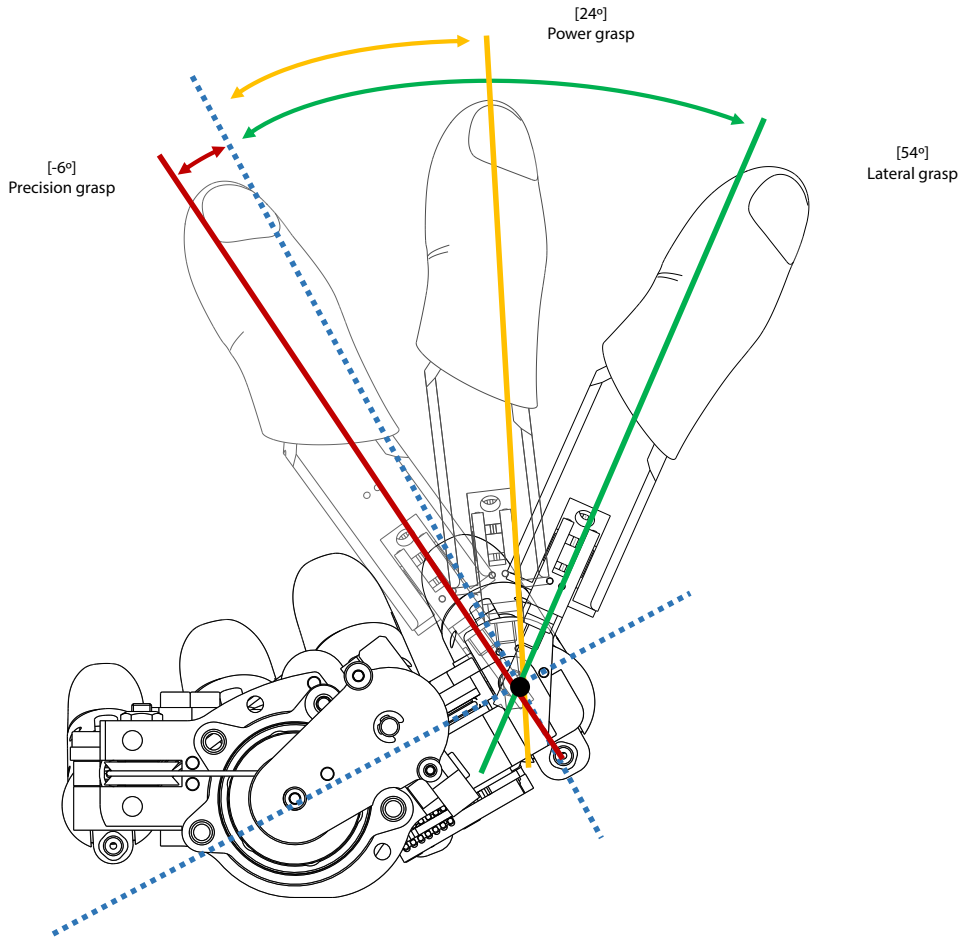

Fig. S2. The three stable rotation positions of the thumb. This digit can be positioned in abduction/adduction in three equally spaced stable positions along an ROM of approximately 60°. These positions are stabilized by using a custom spring-based mechanical plunger integrated in the metacarpal phalanx of the robotic thumb. The tip of the mechanical plunger has an appropriate shape in order to engage with its female counterpart that is machined in the palm frame.

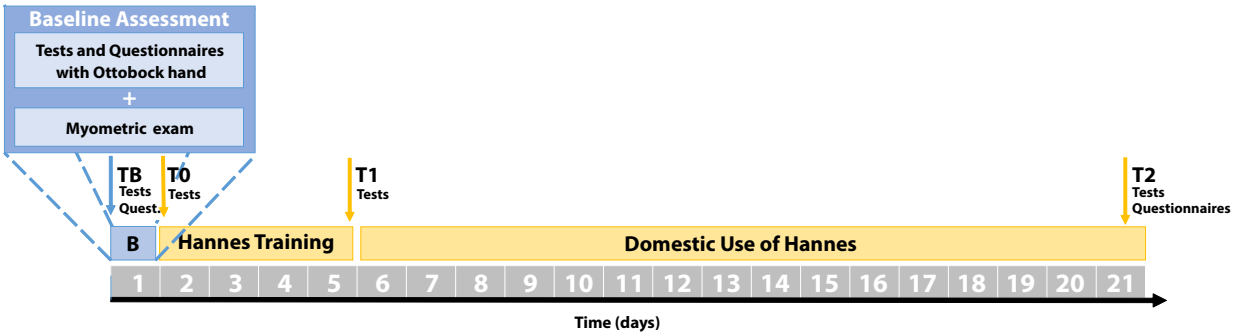

Fig. S3. Outline of the experimental protocol. "B" (day 1) refers to the baseline phase, during which the tests and questionnaires are executed with the reference prosthetic hand (TB) and then the subject receives myometric exams for setting the EMG electrode positions of the Hannes hand. This phase is followed by Hannes training (days 2-5), which begins with tests of Hannes (T0) and terminates with other tests (T1). Finally, the subject brings Hannes home for domestic use (days 6-21) and undergoes a final test and questionnaire phase (T2).

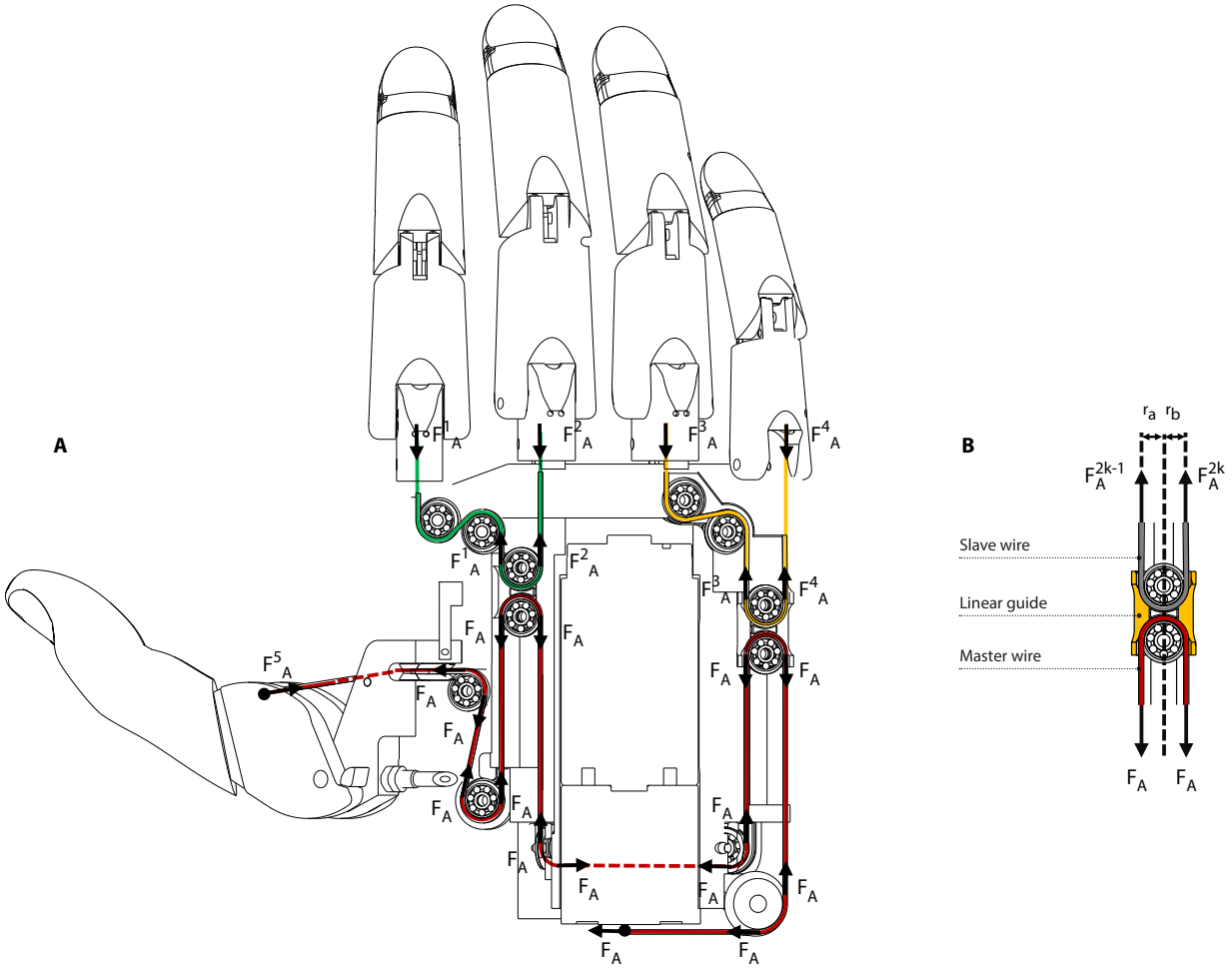

Fig. S4. Forces acting in the palm mechanism. (**A**) Schematic showing the distribution of forces, which results from the tension applied by the leader and follower wires, and (**B**) detail of the custom-made bush bearing.

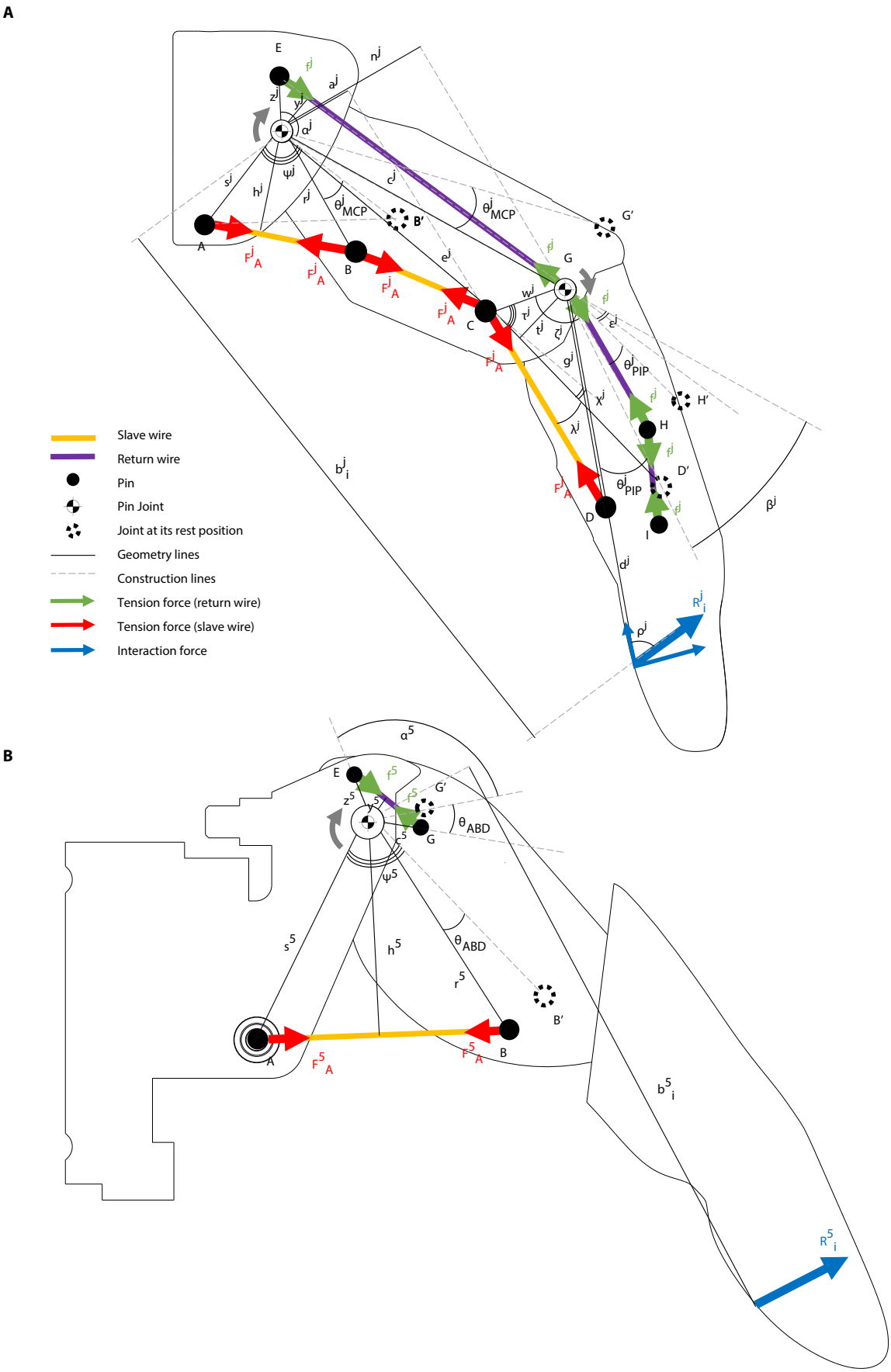
A
B
Slave wire
Return wire
Pin
Pin Joint
Joint at its rest position
Geometry lines
Construction lines
Tension force (return wire)
Tension force (slave wire)
Interaction force

Fig. S5. Mechanics of the digits. (**A**) The finger and (**B**) the thumb. Points A, B, C, D, E, G, H and I represent the axes of the dowel pins employed to guide the wire through the finger, whereas points B', D', G', and H' are the axes at their rest position. The yellow line denotes the wire entering the digits, whereas the purple line represents the return wire. Approximations have been made in the calculations that neglect the radius of the pins because of their small significance in the computation of the MCP and PIP torques. The lever arms upon which the forces act, i.e., $a^j, n^j, h^j, y^j, and\ b_i^j$, can be expressed as follows as a function of the digits' angles:

$$a^j = e^j\ sin\left(\chi^j + \lambda^j\right) \text{ where } \lambda^j = \frac{\pi}{2} - \tau^j - tan^{-1}\left(\frac{\frac{w^j}{g^j} - cos\left(\zeta^j - \theta_{PIP}^j\right)}{sin\left(\zeta^j - \theta_{PIP}^j\right)}\right);$$

$$n^j = c^j\ sin\left(\varepsilon^j + \theta_{PIP}^j\right);$$

$$h^j = s^j\ cos\left(tan^{-1}\left(\frac{\frac{s^j}{r^j} - cos\left(\psi^j - \theta_{MCP}^j\right)}{sin\left(\psi^j - \theta_{MCP}^j\right)}\right)\right);$$

$$y^j = z^j\ cos\left(tan^{-1}\left(\frac{\frac{z^j}{c^j} - cos\left(\alpha^j + \theta_{MCP}^j\right)}{sin\left(\alpha^j + \theta_{MCP}^j\right)}\right)\right);$$

Finally, $b_i^j = [d^j + c^j\ cos\left(\beta^j + \theta_{PIP}^j\right)]\ sin\left(\rho^j\right) + \ c^j\ [sin\left(\beta^j + \theta_{PIP}^j\right)]\ cos\left(\rho^j\right)$.

The same calculation can be computed for the thumb:

$$h^5 = s^5\ cos\left(tan^{-1}\left(\frac{\frac{s^5}{r^5} - cos\left(\psi^5 - \theta_{ABD}\right)}{sin\left(\psi^j - \theta_{ABD}\right)}\right)\right);$$

$$y^5 = z^5\ cos\left(tan^{-1}\left(\frac{\frac{z^j}{c^j} - cos\left(\alpha^5 + \theta_{ABD}\right)}{sin\left(\alpha^5 + \theta_{ABD}\right)}\right)\right);$$

Finally, $b_i^5 = constant$.

Supplementary Tables

Table S1. The main dimensions of the digits of the human hand and Hannes. The percentage differences are reported in the rightmost column.

		Human hand 25th percentile	Human hand 50th percentile	Human hand 75th percentile	Hannes	(Human – Hannes 50th percentile) [%]
Palm	Depth	58	**61**	66	**59,9**	**1,80**
	Width	86	**89**	91	**88,8**	**0,22**
	Length (from F/E to Middle Crotch)	109	**112**	114	**111,8**	**0,18**
Thumb	Diameter Proximal - Intermediate	25	**28**	30	**28,2**	**-0,71**
	Diameter Intermediate - Distal	20	**23**	25	**23,1**	**-0,43**
	Length From Tip to Crotch	56	**58**	61	**58,1**	**-0,17**
Index	Diameter Proximal - Intermediate	20	**20**	23	**20,2**	**-1,00**
	Diameter Intermediate - Distal	18	**18**	20	**18,1**	**-0,56**
	Length From Tip to Crotch	74	**76**	79	**75,4**	**0,79**
Middle	Diameter Proximal - Intermediate	20	**23**	23	**21,9**	**4,78**
	Diameter Intermediate - Distal	18	**18**	20	**18,6**	**-3,33**
	Length From Tip to Crotch	81	**86**	89	**85,2**	**0,93**
Ring	Diameter Proximal - Intermediate	20	**20**	23	**20,7**	**-3,50**
	Diameter Intermediate - Distal	18	**18**	20	**18,1**	**-0,56**
	Length From Tip to Crotch	79	**81**	84	**79,8**	**1,48**
Little	Diameter Proximal - Intermediate	15	**18**	18	**17,8**	**1,11**
	Diameter Intermediate - Distal	15	**15**	15	**15,3**	**-2,00**
	Length From Tip to Crotch	58	**61**	64	**60,1**	**1,5**

Table S2. Scores of the tests and questionnaires. For each subject, are reported the scores obtained with the reference hand (TB) and with Hannes (T0, T1, T2) as well as the difference between scores recorded at T2 and TB (T2-TB, the scores that indicate an improvement are highlighted in green, the scores that did not change are highlighted in yellow and the scores indicating a deterioration of performances from TB to T2 are highlighted in red).

	Subject #1				Subject #2				Subject #3			
	TB	T0	T1	T2	T2 – TB	TB	T0	T1	T2	T2 – TB	TB	T0	T1	T2	T2 – TB
Minnesota score [s]	137.33 ±15.31	132.00 ±6	125.33 ±8.08	123.67 ±4.04	- 13.66	171.67 ±10.07	181.67 ±20.50	142.33 ±6.43	133.67 ±6.03	-38	140.67 ±10.50	210.00 ±20.30	171.00 ±38.74	166.33 ±10.07	26.66
SHAP (IoF [%])	76	78	71	74	-2	72	66	77	76	4	58	43	62	61	3
Spherical [%]	79	82	77	77	-2	74	82	90	88	14	75	57	76	76	1
Tripod [%]	63	70	60	70	7	44	35	44	53	9	29	24	49	50	21
Power [%]	75	77	65	71	-4	59	53	59	66	7	52	42	57	63	11
Lateral [%]	85	75	73	72	-13	77	68	80	83	6	70	34	58	55	-15
Tip [%]	60	68	65	63	3	70	58	70	65	-5	45	30	55	51	6
Extension [%]	75	78	70	76	1	71	66	78	80	9	67	44	61	69	2
OPUS-UEFS															
Score [%]	96.05	x	x	80.36	-15.69	86.76	x	x	82.5	-4.26	67.5	x	x	88.75	21.25
Usage [%]	67.86	x	x	50	-17.86	60.71	x	x	71.43	10.72	74.07	x	x	71.43	-2.64
DASH															
ADLs [%]	0.8	x	x	2.5	1.7	2.5	x	x	2.5	0	4.3	x	x	10	6.7
WORK [%]	0	x	x	0	0	-	x	x	-	-	0	x	x	18.8	18.8
SPORT [%]	0	x	x	0	0	0	x	x	0	0	-	x	x	-	-
TAPES															
Score [%]	98.3	x	x	93.1	-5.2	88.3	x	x	90.8	2.5	74.1	x	x	76.6	2.5
Final Evaluation score	-	-	-	8/9	-	-	-	-	7/9	-	-	-	-	4/9	-

Table S3. Final evaluation questionnaire.

	Subject #1	***Subject #2***	***Subject #3***
Did you use Hannes as frequently as your usual prosthesis?	Yes	Yes	Yes
Any functional difference in ADLs with respect to your prosthesis?	Yes	Yes	No
Is Hannes comfortable for all-day use?	Yes	Yes	Yes
Was the battery charge sufficient?	No	No	No
Did you feel faster during the task execution while using Hannes?	Yes	Yes	No
Do you think that Hannes might improve the execution of ADLs?	Yes	Yes	No
Are you satisfied with the functionality of the Hannes system?	Yes	Yes	Yes
Are you satisfied with the aesthetic of the Hannes system?	Yes	No	No
Is the weight of Hannes acceptable?	Yes	Yes	Yes

Table S4. Comparison table of commercial and research prosthetic hands. Values in green represent the top three scores obtained for each performance metric. In the adaptive grip column, inherent adaptive grip is valued with higher score as compared to adaptive grip using feedback control. Reported values are retrieved from available literature relative to each device (*35, 38-41, 44, 74-76*) and data from Belter's review work (*4*).

Name	Developer	Weight (g)[¶]	Adaptive Grip	Grip Force[#] (N)			Average Finger MCP flexion speed (°/s)[§]	Achievable Grasps
				Lateral	Power	Precision		
Hannes	IIT - Rehab	480	Y	51	141	75	150	Power, precision, lateral
Michelangelo (*4, 38*)	Ottobock	420	N	70	-	60	87.5	Opposition, lateral, and neutral mode
iLimb Pulse (*4, 40*)	Ossur	523	Y[†]	35	71[‡]	35	75.0	Power, precision, lateral, hook, point
Bebionic (*4, 39*)	Ottobock	588	Y[†]	26	75	36	100	Power, precision, lateral, hook, point
Vanderbilt Hand (*4, 74*)	Vanderbuilt University	546	Y[†]	-	45	29	350	Power, precision, lateral, hook, point
Vincent Hand (*4, 41*)	Vincent Systems	509	Y[†]	-	-	-	92.7	Power, precision, lateral, hook, point
KIT Hand (*35*)	Karlsruhe Institute of Technology	-	Y[†]	-	25	-	110	Hook, Power
SoftHand Pro (*75*)	IIT - ADVR	520	Y	-	76	20	-	Power, precision, lateral
MyHand (*44*)	Prensilia	478	Y	-	70	-	170	Power, precision, lateral, hook, point
Azzurra IH2 (*76*)	Prensilia	640	Y[†]	7	35	-	90	Power, precision, lateral, hook, point

[¶]weight of the device comprising passive prono-supination wrist in its $7^{3/4}$ or medium size; [#]continuous force values; [§]computed as ratio between MCP RoM and time to execute travel; [†]adaptive grip implemented via feedback control; [‡]peak force value 136N, (*4*).

Table S5. Participants' information.* Subject 2 also uses the Michelangelo prosthesis during weekends.

	Subject #1	**Subject #2**	**Subject #3**
Age	62	29	55
Age at amputation	14	23	34
Gender	male	male	male
Missing hand	right	right	right
Level of amputation	medial	medial	distal
Dominant hand	right	right	right
Years of prosthesis use	48	6	20
Years of myoelectric prosthesis use	48	5	19
Commonly used prosthesis	Michelangelo	VariPlus*	VariPlus

Table S6. ADL tasks executed during the rehabilitative training with Hannes.

Full and partial opening/closing of the prosthetic hand
Grasping and manipulating wooden objects of different shape (cubes, cylinders, etc.)
Grasping and manipulating small objects such as buttons or coins
*Grasping, manipulating and releasing cups made of different materials (**i.e**., plastic or glass)*
Laying and clearing a table
Tidying up a room
Utilizing cutlery
Cutting an apple and spreading butter on toast
Utilizing a toothbrush and toothpaste
Opening and closing doors using handles and locking/unlocking doors
Simulated driving (turn the steering wheel, shifting gears)
Utilizing occupational therapy panels with zips and strings
Tying laces
Dressing (shirts, jackets)
Writing with a pen on a sheet of paper
Using a computer keyboard

Supplementary Videos

Movie S1. Amputees performing clinical tests with Hannes. Amputated subject performing the Minnesota Manual Dexterity Test - Placing only (MMDT-P) and the Southampton Hand Assessment Procedure (SHAP). High grasp naturalness and efficacy can be noted in both tests.

Movie S2. Healthy participants performing precision and lateral grasps with Hannes. Healthy subjects performing the Southampton Hand Assessment Procedure (SHAP) and Activities of Daily Living (ADL). Pinch and lateral grasps can be noted in this tests.